On the Design of Near-Optimal Sparse Code Multiple Access Codebooks

Yen-Ming Chen, *Member, IEEE*, and Jian-Wei Chen

***Abstract*— Sparse code multiple access (SCMA) is one of the competitive non-orthogonal multiple access (NOMA) techniques for the next generation of communication systems. In this paper, a systematic construction procedure for the design of SCMA codebooks under various channel environments is proposed in order to achieve near-optimal designs, especially for cases which consider small-scale SCMA parameters. The procedure includes the rotation angle design, the construction of multi-dimensional codebooks, and the design of labelling rules. The detailed design criteria and the related properties are derived and investigated. A low-complexity construction algorithm is further proposed for the cases of fading channels. Numerical results show that the designed SCMA codebooks provide improvements in error performance for all of the considered channel conditions, when compared to the codebooks presented in the prior literature.**

***Index Terms*— Sparse code multiple access (SCMA), non-orthogonal multiple access (NOMA), codebook design, message passing algorithm.**

I. Introduction

IN THIRD and fourth generation communication systems, a series of orthogonal multiple access (OMA) technologies, e.g., code domain multiple access (CDMA) and orthogonal frequency domain multiple access (OFDMA), have been widely adopted. In contrast, for those communication systems in the fifth generation and beyond, higher demands arise, including massive connections, high-level spectrum utilization, and lower latency [1]. Considering limited frequency- and time-domain resource elements (REs), it is difficult for OMA-based schemes to satisfy these critical demands. Consequently, potential techniques have been investigated, including millimeter wave communications, full duplex communications, all-spectrum access, ultra-dense networks (UDN), and non-orthogonal multiple access (NOMA) [2]. Compared to conventional OMA-based schemes, NOMA-based schemes are able to achieve large-scale connectivity, low latency and high spectral efficiency, but, nevertheless, suffer from increased interference and receiver complexity [2].

Various NOMA-based schemes have been investigated in previous literature. The power-domain non-orthogonal multiple access (PD-NOMA) scheme [3] with successive interference cancellation (SIC) on the receiver side was proposed in order to multiplex signals from different user equipment (UE) in the power-domain. In contrast, code-domain NOMA techniques were proposed in order to multiplex signals from different UE by using user-specific spreading sequences. For example, in [4] and [5], the low-density signature (LDS) scheme was devised as a synchronous CDMA system. In addition, the multi-user shared access (MUSA) scheme presented in [6] was devised based on the idea of non-orthogonal transmission and grant-free access. Compared to other code-domain NOMA techniques, the sparse code multiple access (SCMA) technique [7], [8] combines both modulation and spreading procedures. Each UE is assigned with its own dedicated codebook, and the information bits can be directly mapped to a multidimensional codeword from an SCMA codebook. Consequently, the shaping gain for a multidimensional constellation is one of the main foundations of the performance improvement in comparison with the simple repetition of QAM symbols in the LDS scheme [4]. In addition, benefiting from the sparse structures of the codebooks, the message passing algorithm (MPA) detector can be adopted to decode the overlapped codewords under a relatively low computational complexity [9], [10].

The key factor that affects the performance of SCMA lies in the design of the codebooks. Following the first SCMA codebook design reported in [7], [8], several design proposals have been further proposed in recent years [11]–[17]. In [11], the codebooks are designed by maximizing the minimum Euclidean distance (MED) value among the codeword pairs chosen from the mother codebook. An improved error performance can be found from the simulation results under the downlink fading channel. In contrast, the codebooks given in [12] are obtained by maximizing the constrained-input channel capacity. It was verified that an improved error performance can be achieved for cases considering outer codes for AWGN and uplink fading channels. The results reported in [11] and [12] were based on the use of fixed pulse-amplitude modulation (PAM) signal constellations on each RE, while rotation angles were designed to produce the signal points transmitted from/for different UE (referred to as the *sub-constellation* in this paper). Actually, there may be an infinite number of choices for the adopted signal constellations

Manuscript received May 17, 2019; revised September 6, 2019 and December 16, 2019; accepted February 6, 2020. Date of publication February 17, 2020; date of current version May 15, 2020. This work was supported by the Ministry of Science and Technology, Taiwan, under Grant MOST 107-2221-E-110-023-MY3. The associate editor coordinating the review of this article and approving it for publication was D. B. Da Costa. *(Corresponding author: Yen-Ming Chen.)*

Yen-Ming Chen is with the Institute of Communications Engineering, National Sun Yat-sen University, Kaohsiung 80424, Taiwan, and also with the Department of Electrical Engineering, National Sun Yat-sen University, Kaohsiung 80424, Taiwan (e-mail: emerychen.cm@gmail.com).

Jian-Wei Chen was with the Institute of Communications Engineering, National Sun Yat-sen University, Kaohsiung 80424, Taiwan. He is now with the Realtek Semiconductor Corporation, Hsinchu 30076, Taiwan (e-mail: aaa888472@gmail.com).

Color versions of one or more of the figures in this article are available online at http://ieeexplore.ieee.org.

Digital Object Identifier 10.1109/TCOMM.2020.2974213

in the complex signal space. Consequently, the method of searching for suitable constellation points for the construction of codebooks is also an important issue. In [13], the star-QAM (quadrature amplitude modulation) constellation was adopted. The ratio between the inner and the outer PSK (phase shift keying) rings can be adjusted to enhance the search for a suitable signal constellation. In another approach in [14], QPSK (quadrature phase shift keying) signal points are used as a sub-constellation, and the rotation angles which are evenly distributed in 2π intervals, are utilized for the sub-constellations. Lastly, in [17], golden angle modulation (GAM) was utilized to build a multidimensional mother constellation for the SCMA codebooks. Although several designs have been proposed in previous literature, systematic design procedures based on mathematical analysis have not been thoroughly investigated for different channel environments.

In this paper, we investigate the design of near-optimal SCMA codebooks for different channel environments. The main contributions of this paper can be summarized as:

1) The design criteria for the construction of SCMA codebooks have been derived and designed considering the AWGN, uplink and downlink Rayleigh fading channels, respectively.
2) The problems related to the design of the SCMA signal matrix/vector for the uplink and downlink Rayleigh fading channels are respectively formulated as the design of the MISO (multiple-input single-output) [18]–[20] and the SISO (single-input single-output) [21] space-time codes in the fast Rayleigh fading channels. The related properties have also been investigated.
3) A systematic construction procedure is proposed to achieve a near-optimal design, especially for cases which consider small-scale SCMA parameters. The procedure includes the rotation angle design, the construction of codewords based on both single-user observation (SUO) and multiple-user observation (MUO), and the design of labelling rules.
4) A low-complexity construction algorithm called the symbol exchange algorithm (SEA) is proposed for the uplink and downlink fading channels, so that the design of SCMA codebooks which have larger sizes is feasible.
5) Several codebook designs for different channel conditions are provided. Compared to previous works presented in the literature, the designed codebooks are able to provide notable improvements in error performance.

The remainder of this paper is organized as follows: Section II introduces the system model. The basic design methods, as well as the construction procedures for the AWGN channel, are investigated in Section III. The construction procedures for the uplink and downlink Rayleigh fading channels are given in Section IV. Numerical results are provided in Section V. Finally, Section VI concludes this paper.

Notation: Matrices and vectors are set in boldface capital and lowercase letters, respectively. $\mathbb{B}$ and $\mathbb{C}$ respectively denote the binary and complex field. $CN(0,1)$ denotes the zero-mean, unit-variance, circularly symmetric, and complex Gaussian distribution. Superscripts *, $^\top$, and † denote the conjugate, the transpose, and the conjugate transpose, respectively.

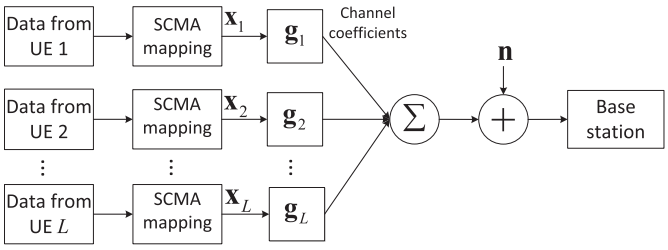

Fig. 1. Block diagram for the uplink SCMA system.

$\|\cdot\|$ denotes the Frobenius norm, $\mathrm{E}[\cdot]$ and $\mathrm{N}[\cdot]$ respectively denote the expectation and normalization functions.

II. System Model

In this paper, we consider both downlink and uplink SCMA systems, which consist of K orthogonal REs and L UEs, and assume that $K < L$. Each UE is able to access d_{v} REs ($d_{\mathrm{v}} < K$), while each RE is shared by d_{f} UEs ($d_{\mathrm{f}} < L$). For each of the SCMA codebooks, we assume that the total number of codewords is M. Consequently, for the l-th UE, the SCMA encoding is defined as the mapping rule

$$f_l : \mathbb{B}^{\log_2 M \times 1} \mapsto \mathcal{X}_l, \quad \text{i.e., } \mathbf{x}_l = f_l(\mathbf{b}_l), \tag{1}$$

where $\mathbf{b}_l \in \mathbb{B}^{\log_2 M \times 1}$ denotes the information vector from/for the l-th UE, and $\mathbf{x}_l \in \mathbb{C}^{K\times 1}$ denotes the SCMA codeword selected from the SCMA codebook $\mathcal{X}_l$ for the l-th UE. We also assume that $\mathrm{E}[\mathbf{x}_l] = d_{\mathrm{v}}$.

For the downlink system, the transmitted vector $\mathbf{y} = [y_1, y_2, \ldots, y_K]^\top \in \mathbb{C}^{K\times 1}$ is obtained by

$$\mathbf{y} = \sum_{l=1}^{L} \mathbf{x}_l. \tag{2}$$

If we let $\mathbf{h}_l \in \mathbb{C}^{K\times 1}$ denote the channel vector from the base station to the l-th UE that has $CN(0,1)$ entries, the received signal at the l-th UE, denoted by $\mathbf{r}_l \in \mathbb{C}^{K\times 1}$, can be written as

$$\mathbf{r}_l = \sqrt{\frac{E_{\mathrm{s}}}{d_{\mathrm{f}}}}\mathrm{diag}\{\mathbf{h}_l\}\mathbf{y} + \mathbf{n}_l, \quad l = 1, 2, \cdots, L, \tag{3}$$

where $\mathbf{n}_l \in \mathbb{C}^{K\times 1}$ denotes the noise vector at the l-th UE that has $CN(0, N_0)$ entries.

In contrast, for the uplink system, the $K \times 1$ received signal vector at the base station can be written as

$$\mathbf{r} = \sqrt{\frac{E_{\mathrm{s}}}{d_{\mathrm{f}}}} \sum_{l=1}^{L} \mathrm{diag}\{\mathbf{g}_l\}\mathbf{x}_l + \mathbf{n}, \tag{4}$$

where $\mathbf{g}_l \in \mathbb{C}^{K\times 1}$ denotes the channel vector from the l-th UE to the base station that has $CN(0,1)$ entries, and $\mathbf{n} \in \mathbb{C}^{K\times 1}$ denotes the noise vector at the base station that has $CN(0, N_0)$ entries. The block diagrams for the two systems can be found in Figs. 1 and 2, respectively.

Since only d_{v} REs are available for the l-th UE, the signal vector $\mathbf{x}_l$ is assumed to be sparse and contains only d_{v} non-zero entries. To effectively design SCMA codebooks for the L UEs, following similar ideas adopted in [11]–[17], a multi-stage design approach is considered in this paper. Let $\mathbf{c}_l$ be

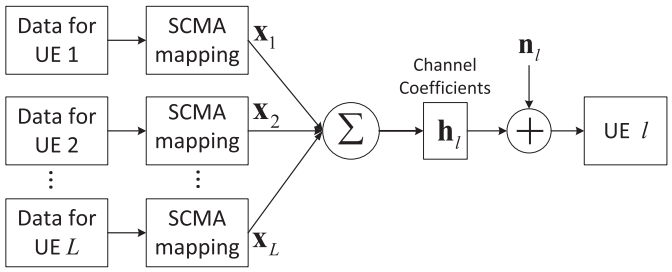

Fig. 2. Block diagram for the downlink SCMA system.

the d_{v}-dimensional complex vector defined within the mother codebook $\mathcal{C}_l \subset \mathbb{C}^{d_{\mathrm{v}}\times 1}$. We further define the mapping

$$g_l : \mathbb{B}^{\log_2 M\times 1} \mapsto \mathcal{C}_l, \quad \text{i.e., } \mathbf{c}_l = g_l(\mathbf{b}_l). \tag{5}$$

The SCMA encoder given in (1) is now re-written as

$$f_l :\equiv \mathbf{V}_l g_l, \quad \text{i.e., } \mathbf{x}_l = \mathbf{V}_l g_l(\mathbf{b}_l), \tag{6}$$

where the $K \times d_{\mathrm{v}}$ matrix $\mathbf{V}_l$ combines the mapping and rotation operations from a d_{v}-dimensional complex codeword from the mother codebook to a K-dimensional complex codeword from an SCMA codebook, when considering the l-th UE. In this paper, we consider the case where $K = 4$, $L = 6$, $d_{\mathrm{v}} = 2$, and $d_{\mathrm{f}} = 3$, and utilize a $K \times L$ factor graph matrix

$$\mathbf{F} = \begin{bmatrix} 0 & 1 & 1 & 0 & 1 & 0 \\ 1 & 0 & 1 & 0 & 0 & 1 \\ 0 & 1 & 0 & 1 & 0 & 1 \\ 1 & 0 & 0 & 1 & 1 & 0 \end{bmatrix}, \tag{7}$$

which is obtained from [22] and [23]. Matrix $\mathbf{F}$ illustrates the locations of the REs which are assigned to different UE. For example, the first column in $\mathbf{F}$ indicates that UE 1 is able to access the second and the fourth REs. Consequently, we define $\mathbf{V}_l \equiv \mathbf{V}'_l\mathbf{\Phi}_l$. The rotation matrix $\mathbf{\Phi}_l$ is defined as

$$\mathbf{\Phi}_l \equiv \mathrm{diag}\{e^{j\phi_{l,1}}, e^{j\phi_{l,2}}, \cdots, e^{j\phi_{l,d_{\mathrm{v}}}}\}, \tag{8}$$

where, in addition, $\mathbf{V}'_l$ for UE l can be generated from the l-th column of $\mathbf{F}$. For example, for UE 1 and UE 2, we have

$$\mathbf{V}'_1 = \begin{bmatrix} 0 & 0 \\ 1 & 0 \\ 0 & 0 \\ 0 & 1 \end{bmatrix} \quad \text{and } \mathbf{V}'_2 = \begin{bmatrix} 1 & 0 \\ 0 & 0 \\ 0 & 1 \\ 0 & 0 \end{bmatrix}. \tag{9}$$

$\mathbf{V}_l$, $l = 3, 4, 5$ and 6, can be generated in a similar way. Lastly, for the receiver design, we adopt the conventional MPA reported in [9] and [10] for multi-user detection.

III. Construction Strategy for Near Optimal SCMA Codebooks on the AWGN Channel

Considering the parameters $K = 4$, $L = 6$, $d_{\mathrm{v}} = 2$, and $d_{\mathrm{f}} = 3$, the matrix $\mathbf{F}'$,

$$\mathbf{F}' \equiv \begin{bmatrix} 0 & \mathcal{S}_1 & \mathcal{S}_2 & 0 & \mathcal{S}_3 & 0 \\ \mathcal{S}_2 & 0 & \mathcal{S}_3 & 0 & 0 & \mathcal{S}_1 \\ 0 & \mathcal{S}_2 & 0 & \mathcal{S}_1 & 0 & \mathcal{S}_3 \\ \mathcal{S}_1 & 0 & 0 & \mathcal{S}_3 & \mathcal{S}_2 & 0 \end{bmatrix}, \tag{10}$$

can be used to demonstrate the following conceptual idea. In the codebook for a single UE, two different *sub-constellations* are considered for the symbols respectively transmitted through two different REs. In contrast, for each of the REs, the signals from/for different UE are chosen from different sub-constellations. We let $\mathcal{A}$ denote the *signal constellation*, which is the set of all possible signal points transmitted through a single RE. $\mathcal{A}$ is formed by considering all possible combinations of three signal points respectively chosen from sub-constellations $\mathcal{S}_1$, $\mathcal{S}_2$, and $\mathcal{S}_3$.

Algorithm 1 SCMA Codebook Construction for the AWGN Channel

1: **Step 1** : Randomly choose d_{f} sub-constellations $\mathcal{S}_i, i = 1, 2, \cdots, d_{\mathrm{f}}$ from the signal sub-constellation pool.
2: **Step 2** : From the perspective of a single RE, optimize the rotation angles $\theta_1^*, \theta_2^*, \cdots$, and $\theta_{d_{\mathrm{f}}}^*$ according to the criterion given in (12).
3: **Step 3** : Based on the SUO reported in Section III-C, for each UE, search and preserve the mother codebooks which achieve the same MED values defined in (14).
4: **Step 4** : Considering the mother codebooks obtained in Step 3, allocate the best combination of codebooks based on the MUO described in Section III-D with the maximum $d_{\min}^{\mathrm{M}}$ value. If some combinations achieve similar $d_{\min}^{\mathrm{M}}$ values, preserve the one with minimum Γ_{AWGN} value provided in (18).
5: **Step 5** : Perform the generalized BSA for the designed codebook for each UE.

Considering the AWGN channel, in this section, we propose a construction strategy for near-optimal SCMA codebooks. The proposed strategy will then be applied to both uplink and downlink fading channels in the next section. The detailed construction procedures are given in Algorithm 1, while the critical steps/algorithms will be introduced in the following subsections.

A. Generation of the Signal Sub-Constellation

In Step 1 of Algorithm 1, we intend to generate a variety of signal sets for the candidates of signal sub-constellations $\mathcal{S}_i, i = 1, 2, \cdots, d_{\mathrm{f}}$. We consider an irregular PAM signal constellation

$$\mathcal{S} = \{-\gamma_{\frac{M-2}{2}}, \cdots, -\gamma_1, -1, 1, \gamma_1, \cdots, \gamma_{\frac{M-2}{2}}\}. \tag{11}$$

In the previous literature [12], [13], considering $M = 4$ the value of γ_1 is set to 3. We build the *signal sub-constellation pool* by using different γ_i values, which provides a sufficient variety of sub-constellation candidates. In addition, all the sub-constellation sets contained in the pool have been normalized, so that an average power value of 1 can be guaranteed for each sub-constellation.

B. Determination of Rotation Angles

Based on d_{f} specific sub-constellations chosen from the signal sub-constellation pool, in Step 2 of Algorithm 1, we determine the optimal rotation angles when applied to the d_{f} signals multiplexed on a single RE. We first let $S_i^{(k)}$ denote the k-th signal point contained in the sub-constellation $\mathcal{S}_i$. Consequently, $A^{(w)} = \sum_{i=1}^{d_{\mathrm{f}}} S_i^{(k_i)} e^{j\theta_i}$ denote the w-th signal point of signal constellation $\mathcal{A}$, where w is a function of k_i,

$i = 1, \cdots, d_{\mathrm{f}}$ and $|\mathcal{A}| = M^{d_{\mathrm{f}}}$. For the optimization of the rotation angles $\theta_1, \theta_2, \cdots$, and $\theta_{d_{\mathrm{f}}}$, we propose minimizing the following metric

$$\{\theta_1^*, \theta_2^*, \cdots, \theta_{d_{\mathrm{f}}}^*\} = \underset{\{\theta_1, \theta_2, \cdots, \theta_{d_{\mathrm{f}}}\}}{\arg\min} \sum_{m=1}^{|\mathcal{A}|-1} \sum_{n=m+1}^{|\mathcal{A}|} \exp(-\|A^{(m)} - A^{(n)}\|^2), \quad (12)$$

which is obtained from the upper bounded error probability of the signal transmission in the AWGN channels, and considers the pair-wise error probabilities of different signal pairs from signal constellation $\mathcal{A}$. It is noted that for the AWGN channel, rather than simply maximizing the MED among signal constellation pairs, taking the number of pairs which achieve the same ED into consideration provides a significant improvement in BER performance for the constructed codebooks in the following procedures. Similar to the case for Step 4 of the algorithm (which will be explained in Section III-D), to simplify the calculation for the metric, the signal-to-noise ratio (SNR) value is set to 1 in (12).

Since the same signal constellations are considered in all REs, the rotation angles θ_i can be optimized by considering only one RE, and then applying the result to different codebooks. If we fix θ_1 as zero, $\theta_2, \theta_3, \cdots, \theta_{d_{\mathrm{f}}}$ can be searched within the range $[0, \pi)$ with a step size of 1 degree. After the optimized $\theta_1^*, \theta_2^*, \cdots, \theta_{d_{\mathrm{f}}}^*$ values are determined, in (8), the values of $\phi_{l,i}$ can thus be ascertained according to the adopted sub-constellations in the codebook for the l-th UE.

C. Design of Mother Codebooks Based on Single-User Observation (SUO)

In Step 3 of Algorithm 1, the considered mother codebooks $\mathcal{C}_l$, $l = 1, 2, \cdots, L$, are assumed to be equal-sized. Consequently, for each mother codebook, we require M length-d_{v} codewords. If we let $d_{\mathrm{v}} = 2$, two different signal sub-constellations, say $\mathcal{S}_i$ and $\mathcal{S}_j$, $i \neq j$, should be respectively adopted for the two REs accessed by a single UE, and will be used for the construction of a mother codebook. Consequently, the design of the mother codebook is equivalent to determining the best approach to signal pairing for the two signals respectively chosen from $\mathcal{S}_i$ and $\mathcal{S}_j$, following a specific criterion.

At the beginning of the construction, the symbols for the first dimension of the M codewords can be randomly chosen from the M elements of $\mathcal{S}_i$. Accordingly, when we intend to determine the symbols for the second dimension of the M codewords, there will be a total of $T = M!$ pairing methods. Consequently, when determining a mother codebook with d_{v} dimensions, there will be $T = (M!)^{d_{\mathrm{v}}-1}$ possible combinations. For the l-th UE, we let $\mathcal{C}_{l,t}$, $t = 1, 2, 3, \cdots, T$, denote the resultant codebook candidates obtained from the T combination patterns. We further let $d^{\mathrm{S}}_{\min,l,t}$, $t = 1, 2, 3, \cdots, T$, represent the MED value from the $\binom{M}{2}$ codeword pairs chosen from the mother codebook $\mathcal{C}_{l,t}$. Accordingly, we have

$$d^{\mathrm{S}}_{\min,l,t} = \arg\min_{i \neq j} \|\mathbf{c}_{l,t}^{(i)} - \mathbf{c}_{l,t}^{(j)}\|, \quad (13)$$

where $\mathbf{c}_{l,t}^{(i)} \in \mathbb{C}^{d_{\mathrm{v}} \times 1}$ represents the i-th codeword in the mother codebook $\mathcal{C}_{l,t}$ for the l-th UE. Based on the observation for the minimum distance, we have

$$\mathcal{C}_l^* = \arg \max_{t=1,2,\cdots,T} d^{\mathrm{S}}_{\min,l,t}, \quad (14)$$

where $\mathcal{C}_l^*$ is chosen for the adopted mother codebook for the l-th UE. According to (6), the transmitted signal vector $\mathbf{x}_l$ is produced from the phase rotation of the codewords in the mother codebook. It is worth mentioning that the phase rotation does not change the distance values for the codeword pairs, and the two operations can be designed separately.

When individually optimizing the codebooks for different UE, it is observed that several codebook candidates actually achieve the same MED values according to (13). In addition, the transmitted codewords from different UE are multiplexed on different REs. If we focus on the combined transmitted signal vector $\mathbf{y}$, which is formed across K REs, signal vector pairs that have small ED values may still be induced, even if codebooks that achieve $d^{\mathrm{S}}_{\min}$ values are respectively adopted for different UE. Consequently, by designing the mother codebooks separately for different UE, we may not be able to achieve a globally optimized error performance. Rather than using the mother codebook obtained according to (13) and (14) for each UE, we preserve the mother codebooks which produce the same MED values, and use them for the design of mother codebooks based on MUO.

D. Design of Mother Codebooks Based on Multiple-User Observation (MUO)

After performing the design process outlined in Section III-C, we denote the α_l preserved mother codebooks for the l-th UE as $\mathcal{C}_{l,t}$, $l = 1, 2, \cdots, L$, $t = 1, 2, \cdots, \alpha_l$. We focus on the t_l-th mother codebook for the l-th UE and assume that the k_l-th codeword is transmitted, where $t_l \in \{1, 2, \cdots, \alpha_l\}$ and $k_l \in \{1, 2, \cdots, M\}$. The i-th transmitted signal vector $\mathbf{y}^{(i)}$, where i is a function of k_l, $l = 1, 2, \cdots, L$, can be expressed as

$$\mathbf{y}^{(i)}_{t_1,t_2,\cdots,t_L} = \sum_{l=1}^{L} \mathbf{V}_l \mathbf{c}_{l,t_l}^{(k_l)}. \quad (15)$$

Consequently, the ED $d^{\mathrm{M}}_{i,j,t_1,t_2,\cdots,t_L}$ between transmitted signal vectors $\mathbf{y}^{(i)}_{t_1,t_2,\cdots,t_L}$ and $\mathbf{y}^{(j)}_{t_1,t_2,\cdots,t_L}$ is defined as

$$d^{\mathrm{M}}_{i,j,t_1,t_2,\cdots,t_L} = \|\mathbf{y}^{(i)}_{t_1,t_2,\cdots,t_L} - \mathbf{y}^{(j)}_{t_1,t_2,\cdots,t_L}\|. \quad (16)$$

For all the $\binom{M^L}{2}$ possible transmitted signal vectors, the MED is defined as

$$d^{\mathrm{M}}_{\min,t_1,t_2,\cdots,t_L} = \arg\min_{i \neq j} d^{\mathrm{M}}_{i,j,t_1,t_2,\cdots,t_L}. \quad (17)$$

In addition, if we sort all possible $d^{\mathrm{M}}_{i,j,t_1,t_2,\cdots,t_L}$ values in an ascending order with the index parameter u, and denote the results as $\hat{d}^{\mathrm{M}}_u$, we are able to calculate the metric

$$\Gamma_{\mathrm{AWGN},t_1,t_2,\cdots,t_L} = \mathrm{N}\left[\sum_{u=1}^{\beta} N_u \exp(-(\hat{d}^{\mathrm{M}}_u)^2)\right], \quad (18)$$

where N_u denotes the number of codeword pairs which guarantee a distance value of $\hat{d}^{\mathrm{M}}_u$. Similarly, the metric Γ_{AWGN} is obtained from the upper bounded error probability for the

transmission of signal vector on the AWGN channel. It is noted that for the calculation of Γ_{AWGN}, we only consider the first β smallest distance values. The value of β is set as 2 to 3% of the number of possible $\hat{d}_u$ values, which is supposed to be sufficient for reflecting the level of error probability.

Consequently, using the preserved mother codebooks $\mathcal{C}_{l,t}$, $t = 1, 2, \cdots, \alpha_l$, for the l-th UE, $l = 1, 2, \cdots, L$, we have a total of $\prod_l \alpha_l$ possible combination patterns for the adopted codebooks. The most important target in our system design is to improve the BER performance in the high-SNR region. Consequently, we obtain the designed mother codebooks by first considering

$$\{\mathcal{C}_1^*, \mathcal{C}_2^*, \cdots, \mathcal{C}_L^*\} = \arg \max_{t_l \in \{1,2,\cdots,\alpha_l\}} d^{\mathrm{M}}_{\min, t_1, t_2, \cdots, t_L}. \quad (19)$$

Moreover, if several possible combinations achieve very similar $d^{\mathrm{M}}_{\min, t_1, t_2, \cdots, t_L}$ values, we choose the one that satisfies

$$\{\mathcal{C}_1^*, \mathcal{C}_2^*, \cdots, \mathcal{C}_L^*\} = \arg \min_{t_l \in \{1,2,\cdots,\alpha_l\}} \Gamma_{\mathrm{AWGN}, t_1, t_2, \cdots, t_L}, \quad (20)$$

which helps us to focus on improving the BER performance in the low-SNR region. Accordingly, in (18), we set the SNR value to 1 (0 dB) for the convenience of reflecting the performance of the system in a relatively low-SNR region.

E. Design of Labelling Rules for SCMA Codebooks

After performing the design process described in Section III-C, the L mother codebooks for the UEs can be obtained. However, for each of the mother codebooks, we only construct its M codewords, but have not defined the corresponding labelling bits for the codewords.

In various early works involving signal modulation strategies, Gray mapping is usually considered as the optimal labelling rule [24], [25], since the bit differences between the nearest constellation points can be minimized. In Step 6 of Algorithm 1, the BSA reported in [26], [27] is generalized to the SCMA scheme to determine the bit labelling rules for the L codebooks. Let $\mathcal{C}_l^*$ denote the decided mother codebook for the l-th UE. Under the AWGN channel, the labelling rule ξ_l should be designed to minimize the metric

$$\Xi(\xi_l) \equiv \sum_{i=1}^{M-1} \sum_{j=i+1}^{M} N_{i,j}(\xi_l) \exp(-d^2_{l,i,j}), \quad (21)$$

where $N_{i,j}(\xi_l)$ represents the number of different labelling bits between $\mathbf{c}_l^{(i)}$ and $\mathbf{c}_l^{(j)}$, based on the considered labelling rule ξ_l, and $d_{l,i,j}$ is defined as $\|\mathbf{c}_l^{(i)} - \mathbf{c}_l^{(j)}\|$.

In the BSA-based labelling design for an SCMA codebook, we first randomly assign different labelling bits to M codewords, and initialize the labelling rule ξ and its cost value $\Xi(\xi)$ based on (21). Starting from the first codeword, we test all possible switches for the assigned labelling bits with other codewords in order to obtain new labelling rules. For each new labelling rule ξ_{sw}, if $\Xi(\xi_{\mathrm{sw}})$ is larger than $\Xi(\xi)$, it implies that the error performance may become worse after the switch, and we need to switch back the labelling bits between the two codewords. Otherwise, we retain this switch, update ξ and $\Xi(\xi)$ using ξ_{sw} and $\Xi(\xi_{\mathrm{sw}})$, respectively, and re-test all possible switches in sequence. If all the possible switches have been tested without any switch occurring, we retain the labelling bits for the first codeword, and then repeat the entire process from the second codeword. Refer to [26] and [27] for more details about the BSA.

Lastly, Algorithm 1 can be executed several times by using different selections from the signal sub-constellation pool to achieve a near-optimal codebook design. A topic in our future research will be to develop a fast algorithm that can preliminary determinate the combination of sub-constellations which will more probably achieve a satisfactory codebook design.

IV. Construction Strategy for Near Optimal SCMA Codebooks on Rayleigh Fading Channels

In this section, we generalize the proposed design process for the case of AWGN channel into two different scenarios. The cases when considering the uplink and downlink Rayleigh fading channels are investigated in Sections IV-A and IV-B, respectively. To prevent the need to repeat the contents, parameters similar to those used in Section III will be adopted without re-definition.

A. SCMA Scheme for Uplink Rayleigh Fading Channels

When considering the uplink Rayleigh fading channel, if we focus on a single RE and regard the signals from different UE as signals transmitted from different transmit antennas, the SCMA scheme can be regarded as a MISO system that has d_{f} transmit antennas and a single receive antenna. In addition, if we regard different REs as different time indices, the design of the SCMA signal matrix is actually equivalent to the design of a $d_{\mathrm{f}} \times K$ space-time code on the fast Rayleigh fading channels [18], [19].

We let $\mathbf{s}_k \equiv [x_{l_1,k}, x_{l_2,k}, \cdots, x_{l_{d_{\mathrm{f}}},k}]^\top$ denote the transmit signal vector at the k-th RE, where $x_{l_1,k}$ denotes the transmit symbol from the l_1-th UE at the k-th RE, and $l_1, l_2, \cdots, l_{d_{\mathrm{f}}}$ denote the indices of the UEs which access the k-th RE. If we define r_k as the k-th element in $\mathbf{r}$, Equation (4) can be reformulated as

$$r_k = \sqrt{\frac{E_{\mathrm{s}}}{d_{\mathrm{f}}}} \sum_{i=1}^{d_{\mathrm{f}}} g_{l_i,k} x_{l_i,k} + n_k, \quad (22)$$

where element $g_{l_i,k}$ denotes the $CN(0,1)$ distributed channel coefficient between the l_i-th UE that accesses the k-th RE and the base station. Since the indices $l_1, l_2, \cdots, l_{d_{\mathrm{f}}}$ vary in different REs, the channel coefficient $g_{l_i,k}$ varies in different l_i and k values, and can be regarded as a fast Rayleigh fading MISO channel.

Define $\mathbf{S} \equiv [\mathbf{s}_1, \mathbf{s}_2, \cdots, \mathbf{s}_K]$. Based on the result reported in [19], the upper bound of the pair-wise error probability (PEP) between two possible transmit signal matrices $\mathbf{S}$ and $\hat{\mathbf{S}}$ can be derived under the assumption of a high SNR, and is written as

$$\begin{aligned} \mathbf{P}(\mathbf{S} \to \hat{\mathbf{S}}) &\le \prod_{k \in \rho(\mathbf{S}, \hat{\mathbf{S}})} |\mathbf{s}_k - \hat{\mathbf{s}}_k|^{-2} \left(\frac{E_{\mathrm{s}}}{4 d_{\mathrm{f}} N_0}\right)^{-\delta} \\ &= d_{\mathrm{p}}^{-2} \left(\frac{E_{\mathrm{s}}}{4 d_{\mathrm{f}} N_0}\right)^{-\delta}, \end{aligned} \quad (23)$$

where $\rho(\mathbf{S},\hat{\mathbf{S}})$ denotes the set of RE indices in which $\mathbf{s}_k \neq \hat{\mathbf{s}}_k$, and $\delta \equiv |\rho(\mathbf{S},\hat{\mathbf{S}})|$. In addition, d_{p}^2 denotes the *product distance* (PD) between the two signal vectors, and is given by

$$d_{\mathrm{p}}^2 = \prod_{k\in\rho(\mathbf{S},\hat{\mathbf{S}})} |\mathbf{s}_k - \hat{\mathbf{s}}_k|^2. \tag{24}$$

Following the design criteria for space-time coding [18]–[20], the most important criterion for minimizing the PEP is to maximize the minimum value of δ among all possible $(\mathbf{S},\hat{\mathbf{S}})$ pairs. However, for an SCMA scheme that assumes d_{v} accessible REs for each UE, it is easy to verify that the minimum value of δ is fixed as d_{v}. Moreover, cases where $\delta = d_{\mathrm{v}}$ occur if, and only if, one of the UEs transmits two different codewords in $\mathbf{S}$ and $\hat{\mathbf{S}}$, respectively, while all of the other UEs transmit the same codeword. In other words, in (23), $\rho(\mathbf{S},\hat{\mathbf{S}})$ contains only d_{v} RE indices for this case, and any two vectors $\mathbf{s}_k$ and $\hat{\mathbf{s}}_k$ only differ in one element, $\forall k \in \rho(\mathbf{S},\hat{\mathbf{S}})$. As a result, the second design criterion, in which the minimum product distance (MPD) for the entire signal matrix is maximized when $\delta = d_{\mathrm{v}}$, is actually equivalent to individually maximizing the MPDs for the mother codebooks for the UEs. For the mother codebook design based on SUO, similar to the case for the AWGN channel, there will be $T = (M!)^{d_{\mathrm{v}}-1}$ possible candidates for the mother codebook. Accordingly, for the i-th and the j-th codewords from the t-th codebook candidate, we define the product distance as

$$d_{\mathrm{p},l,t,i,j}^2 = \prod_{k=1}^{d_{\mathrm{v}}} |c_{l,t,k}^{(i)} - c_{l,t,k}^{(j)}|^2, \tag{25}$$

where $c_{l,t,k}^{(i)}$ denotes the k-th symbol in the i-th codeword $\mathbf{c}_{l,t}^{(i)}$ of the mother codebook $\mathcal{C}_{l,t}$ for the l-th UE.

We sort all possible $d_{\mathrm{p},l,t,i,j}^{\mathrm{S}}$ values in an ascending order using the index parameter u, and denote the results as $\hat{d}_{\mathrm{p},l,t,u}^{\mathrm{S}}$. Considering also the number of codeword pairs which provide the same PD value, we can calculate the metric

$$\Psi_{l,t} = \mathrm{N}\left[\sum_{u} N_u \frac{1}{\hat{d}_{\mathrm{p},l,t,u}^2}\right], \tag{26}$$

Consequently, the designed mother codebook for the l-th UE is given by

$$\mathcal{C}_l^* = \arg \min_{t=1,2,\cdots,T} \Psi_{l,t}. \tag{27}$$

In [29], based on an optimization method, the authors have shown that the optimal signal sub-constellation for uplink Rayleigh channels is the QPSK constellation for the case where $M = 4$. In addition, for the steps in the rotation angle design and the codebook design based on MUO, we have the following propositions:

Proposition 1: For the uplink Rayleigh fading channels, the design of the rotation angles is not required and does not affect the error performance.

Proof: The proof can be found in Appendix A. ∎

Proposition 2: For the uplink Rayleigh fading channels, a codebook design based on MUO is not required and does not affect the error performance, when considering symmetrical signal sub-constellations.

Proof: The proof can be found in Appendix B. ∎

Algorithm 2 SCMA Codebook Construction for the Uplink Rayleigh Fading Channel

1: **Step 1** : Choose identical signal sub-constellations for $\mathcal{S}_i, i = 1,2,\cdots,d_{\mathrm{f}}$. For the case where $M = 4$, use the QPSK constellation.
2: **Step 2** : Based on SUO, search the mother codebook for each UE according to (27).
3: **Step 3** : Perform a generalized BSA for the designed codebook for each UE, and use the design metric given in (28).

Consequently, in the next step, the BSA is used to design the labelling rule. Considering both the PD values for the codeword pairs and the number of neighbors, following a similar definition of the parameters, the labelling rule ξ_l should be designed by minimizing the metric

$$\Xi(\xi_l) \equiv \sum_{i=1}^{M-1}\sum_{j=i+1}^{M} N_{i,j}(\xi_l)\frac{1}{d_{\mathrm{p},l,i,j}^2}. \tag{28}$$

Lastly, the overall construction procedure is given in Algorithm 2.

B. SCMA Scheme for Downlink Rayleigh Fading Channels

In contrast to the case for the uplink channel, when considering the downlink Rayleigh fading channel, the transmit signals for different UEs are first combined and then sent to the channel on each UE. If we regard different REs as different time indices, the design of the combined SCMA signal vector is actually equivalent to the design of the coded signal vector on the SISO fast Rayleigh fading channel [21].

Considering the system model given in (3), since the channel coefficient $h_{l,k}$, which is the k-th element of $\mathbf{h}_l$, varies for each different RE index k, it can be regarded as a fast Rayleigh fading channel. Following the result provided in [21], the upper bound of the PEP between two possible transmit signal vectors $\mathbf{y}$ and $\hat{\mathbf{y}}$ can be derived under the assumption of a high SNR, and is given by

$$\begin{aligned}\mathbf{P}(\mathbf{y}\rightarrow\hat{\mathbf{y}}) &\leq \prod_{k\in\rho(\mathbf{y},\hat{\mathbf{y}})} |y_k - \hat{y}_k|^{-2}\left(\frac{E_{\mathrm{s}}}{4N_0}\right)^{-\delta} \\ &= d_{\mathrm{p}}^{-2}\left(\frac{E_{\mathrm{s}}}{4N_0}\right)^{-\delta},\end{aligned} \tag{29}$$

where $\rho(\mathbf{y},\hat{\mathbf{y}})$ denotes the set of RE indices in which $y_k \neq \hat{y}_k$, and $\delta \equiv |\rho(\mathbf{y},\hat{\mathbf{y}})|$. In addition, d_{p}^2 denotes the PD between the two signal vectors, and is given by

$$d_{\mathrm{p}}^2 \equiv \prod_{k\in\rho(\mathbf{y},\hat{\mathbf{y}})} |y_k - \hat{y}_k|^2. \tag{30}$$

Unlike the uplink channel, the calculation of the PD value for a combined signal vector pair involves the combined signals y_k and $\hat{y}_k$ on the RE. To maximize the PD value, the MED between any two possible combined signal points

on each RE should be maximized. Consequently, the design process for the rotation angles is similar to that for the AWGN channel, but, however, is aimed at maximizing the MED of the combined signal point pairs. Accordingly, we replace (12) with the following equation:

$$\{\theta_1^*, \theta_2^*, \cdots, \theta_{d_\mathrm{f}}^*\} = \underset{\{\theta_1, \theta_2, \cdots, \theta_{d_\mathrm{f}}\}}{\arg\max} \min_{m \neq n} \|A^{(m)} - A^{(n)}\|. \quad (31)$$

The rotation angles should be properly designed such that the MED for the combined signal constellation is not equal to zero. As a result, similar to the case for the uplink channel, the minimum value of δ would be fixed to d_v. The cases where $\delta = d_\mathrm{v}$ would occur if, and only if, one of the UEs transmits two different codewords in $\mathbf{y}$ and $\hat{\mathbf{y}}$, respectively, while all other UEs transmit the same codeword. Consequently, the design process for the mother codebooks based on SUO is the same as that for the uplink channel. To maximize the PD value for a single mother codebook, the QPSK signal constellation is still optimal for the signal sub-constellations.

The design for mother codebooks based on SUO optimizes the design metric for cases where $\delta = d_\mathrm{v}$. *Proposition* 2 reveals that for the uplink fading channel, considering the design based on MUO, i.e., those cases where $\delta > d_\mathrm{v}$, does not change the error performance. However, on the downlink channel, since the calculation of the PD involves the combined signals on the REs according to (30), engaging MUO still helps in improving the error performance. It is also noted that, based on (29), optimizing the design metric for cases where $\delta = d_\mathrm{v}$ is sufficient to provide satisfactory error performance in the high-SNR region. However, performing the codebook design based on MUO is able to improve the error performance in the low- and middle-SNR region. Accordingly, we perform a design process based on MUO which is similar to that reported in Section III-D. For a signal vector pair $(\mathbf{y}^{(i)}_{t_1,t_2,\cdots,t_L}, \mathbf{y}^{(j)}_{t_1,t_2,\cdots,t_L})$, we replace (16) with (37), where (37) is shown in the bottom of page 10. In addition, Equations (18) and (20) are respectively replaced with the following two equations

$$\Gamma^{(\delta)}_{\mathrm{DL},t_1,t_2,\cdots,t_L} = \mathrm{N}\left[\sum_u N_u \frac{1}{(\hat{d}^{\mathrm{M}}_{\mathrm{p},u})^2}\right], \quad (32)$$

$$\{\mathcal{C}_1^*, \mathcal{C}_2^*, \cdots, \mathcal{C}_L^*\} = \arg \min_{t_l \in \{1,2,\cdots,\alpha_l\}} \Gamma^{(\delta)}_{\mathrm{DL},t_1,t_2,\cdots,t_L}. \quad (33)$$

It is noted that in (32), we only focus on the signal pairs which satisfy a specific δ value. Lastly, we perform the generalized BSA for the labelling rule design using the same metric as that for the uplink fading channel. The detailed design procedure can be found in Algorithm 3.

C. Low-Complexity Design Method for High-Rate Codebooks

For the uplink Rayleigh fading channel, it has been revealed that the step based on the MUO can be removed without introducing any loss in error performance. In addition, for the downlink Rayleigh fading channel, the MUO step can also be safely removed if we carefully design the rotation angles and only focus on the BER performance in the high-SNR region. In contrast, performance degradation would be induced if we ignore the MUO step for the AWGN channel.

Algorithm 3 SCMA Codebook Construction for the Downlink Rayleigh Fading Channel

1: **Step 1** : Choose identical signal sub-constellations for $\mathcal{S}_i, i = 1, 2, \cdots, d_\mathrm{f}$. For the case where $M = 4$, use the QPSK constellation.
2: **Step 2** : From the perspective of a single RE, optimize the rotation angles $\theta_1^*, \theta_2^*, \cdots$, and $\theta_{d_\mathrm{f}}^*$ according to the criterion given in (31).
3: **Step 3** : Based on SUO, for each UE, search and preserve the mother codebooks which produce the same Ψ values defined in (26).
4: **Step 4** : Allocate the best combination of the mother codebooks using MUO. Preserve the codebook with the minimum $\Gamma_{\mathrm{DL}}^{(d_\mathrm{v}+1)}$ value provided in (32). If the codebooks produce similar $\Gamma_{\mathrm{DL}}^{(d_\mathrm{v}+1)}$ values, preserve the one with the minimum $\Gamma_{\mathrm{DL}}^{(d_\mathrm{v}+2)}$ value, and so on.
5: **Step 5** : Perform the generalized BSA for the designed codebook for each UE, and use the design metric given in (28).

When considering high-rate codebook designs with increased modulation order M, the complexity level will be significantly increased when considering the proposed near-optimal algorithms. Inspired by the fact that the MUO step can be removed for Rayleigh fading channels, the codebook design based on SUO in combination with the labelling design process is merged into a single step in order to reduce the design complexity. In Algorithm 4, a symbol exchange algorithm (SEA) is proposed that efficiently constructs SCMA codebooks with a more reasonable complexity level. The modified design process is described as follows. The step for the rotation angle design will still be performed when considering downlink channels. However, the SUO and labelling design steps will be combined to the SEA reported in Algorithm 4. At the beginning, we randomly assign the labelling bits and modulation symbols for the M codewords within a codebook. Rather than switching the labelling bits, we fix the labelling bits and the symbols in the first dimension of the codewords, and then exchange the remaining symbols between codeword pairs, following a similar method as that of the BSA-based labelling design algorithm. The SEA algorithm can be performed several times using different initial conditions to prevent it from falling into the local optimum region.

If we skip the MUO step, the crucial procedure which dominates the complexity level is the calculation of the similar metric contained in equations (26) and (28). Consequently, considering the proposed near-optimal algorithm, if we use the number of calculations to denote the complexity level, it is dominated by the search for the codebooks for individual users, and is $8! = 40320$ when considering $M = 8$. In contrast, the average number of calculations in SEA is about 8404, and a 79.6% reduction in computational complexity can be achieved. The reduction in complexity level reaches 99% when considering $M = 16$. Consequently, when considering fading channels, the proposed SEA mitigates the complexity level as the size of the codebook M increases, and, hence, can be applied to the design for moderate or large-sized codebooks.

Algorithm 4 Symbol Exchange Algorithm (SEA)

Input: Randomly choose the symbols for each dimension of the M codewords from the M elements of the related sub-constellations. Randomly assign the labelling bits for the M codewords.
Fix the symbols in the first dimension of all codewords. Calculate $\Xi_{\rm ini}$ using (28).
for $k = 2 : d_{\rm v}$ **do**
  for $i = 1 : M-1$ **do**
    for $j = i+1 : M$ **do**
      In the k-th dimension, switch the symbol of the i-th codeword with that of the j-th code- word.
      Calculate the metric $\Xi_{\rm sw}$ using (28).
      if $\Xi_{\rm sw} < \Xi_{\rm ini}$ **then**
        Retain the switch and update $\Xi_{\rm ini}$ with $\Xi_{\rm sw}$.
        Set $j = i+1$. **Go to** 6.
      else
        Switch back the two symbols.
      End if
    End for k, i, and j
Output: The constructed mother codebook for a single UE.

TABLE I
COMPARISON OF VARIOUS SCHEMES CONSIDERING THE AWGN CHANNEL WHERE $M = 4$

Scheme	$d^{\rm M}_{\rm min}$	$\Gamma_{\rm AWGN}$
Example 1	1.51	0.2152
CB [12]	1.15	0.2448
HUA [15]	0.707	0.2457
CR [14]	1.16	0.2823
SQ [13]	1.0272	0.3276

V. SIMULATION RESULTS

In this section, we consider the cases where parameters $L = 6$, $K = 4$ $d_{\rm v} = 2$, and $d_{\rm f} = 3$. The details of the designed SCMA codebooks under various channel environments are given in Appendix C. The definition of the $\frac{E_b}{N_0}$ value is given by

$$\frac{E_b}{N_0} = \frac{E_s}{N_0} \cdot \frac{1}{d_{\rm f} \cdot \log_2 M}, \tag{34}$$

where $\frac{E_s}{N_0}$ is the SNR value for each RE by definition. We first focus on the case which operates on the AWGN channel, and compare the proposed scheme with several schemes reported in previous literature, where the same channel condition is considered.

It is shown in Table I and Fig. 3 that the design metrics $d^{\rm M}_{\rm min}$ and $\Gamma_{\rm AWGN}$ are sufficient for managing the error performance for the AWGN channel environment. The level of the BER value in the low-SNR region is proportional to the design metric $\Gamma_{\rm AWGN}$, which is dominated by the numbers of nearest signal vector pairs. In contrast, the level of the BER value in the high-SNR region is related to both $d^{\rm M}_{\rm min}$ and $\Gamma_{\rm AWGN}$.

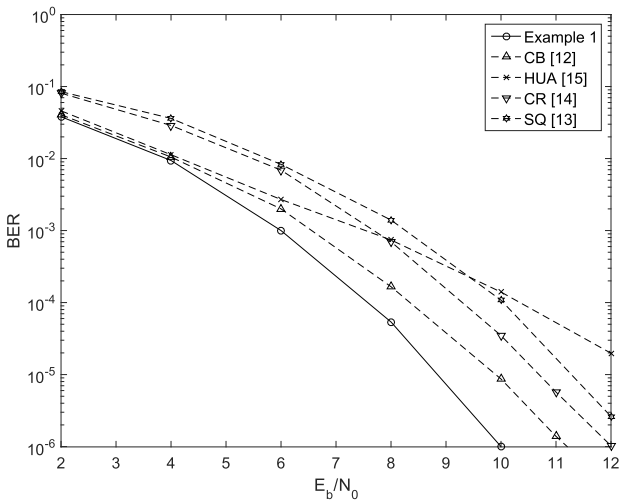

Fig. 3. BER performance versus the E_b/N_0 value for the AWGN channels where $M = 4$.

TABLE II
COMPARISON OF VARIOUS SCHEMES CONSIDERING THE UPLINK RAYLEIGH FADING CHANNEL

$M = 4$	$d^{\rm M}_{\rm min}$	Ψ	$M = 8$	Ψ
Example 2	0	0.1667	Circular-QAM	0.3797
GAM [17]	0.7122	0.2008	APSK	0.3348
HUA [15]	0.707	0.3060	Triangular-QAM	0.3336
CB [12]	1.15	0.3109	GAM [17]	0.4399
CS [16]	0.5469	0.7556	Benchmark 1	1.5416
			Benchmark 2	6.8670

The scheme reported in [15] provides a low $\Gamma_{\rm AWGN}$ value, and, hence, achieves a satisfactory BER performance in the low-SNR region. However, a large $d^{\rm M}_{\rm min}$ value is not able to be achieved when considering the MUO analysis for the overall transmit signal vectors, and, hence, a performance degradation is induced in the high-SNR region. In addition, the scheme reported in [14] provides a slightly higher $d^{\rm M}_{\rm min}$ value when compared to that reported in [12]. However, the scheme reported in [14] achieves a much higher $\Gamma_{\rm AWGN}$ value when compared to that achieved in [12]. Consequently, the high-SNR performance reported in [14] is worse than that achieved in [12]. The proposed scheme is able to provide an improvement in performance in both the high- and the low-SNR region, and achieve a gain of 1.34 dB at a BER value of 10^{-6}, when compared to the scheme presented in [12].

The relevant results when considering the uplink Rayleigh fading channel where $M = 4$ are demonstrated in Table II and Fig. 4. In Table II, the Ψ value for the different schemes is obtained by observing an arbitrary mother codebook for a single UE. Comparing the results provided in Table II and Fig. 4, it is shown that the level of the BER value is proportional to the design metric Ψ, however, weakly correlated to the $d^{\rm M}_{\rm min}$ value. It is also interesting to observe that, due to the omission of the rotation angle design, the proposed scheme has a $d^{\rm M}_{\rm min}$ value of 0, but still achieves the best error performance when compared to the benchmark systems. As indicated in Section IV-A,

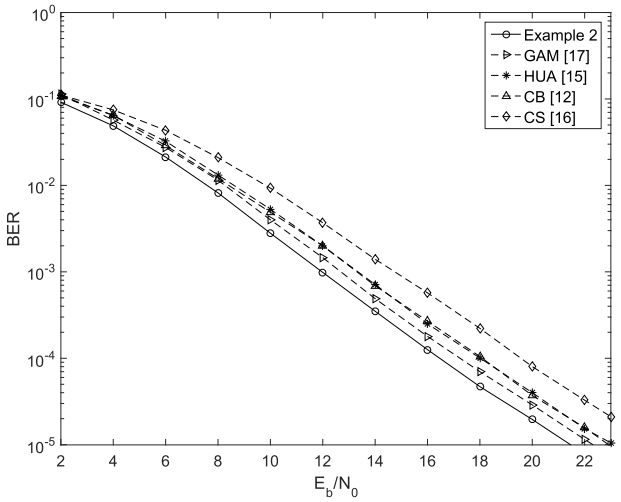

Fig. 4. BER performance versus E_b/N_0 value for the uplink Rayleigh fading channel where $M = 4$.

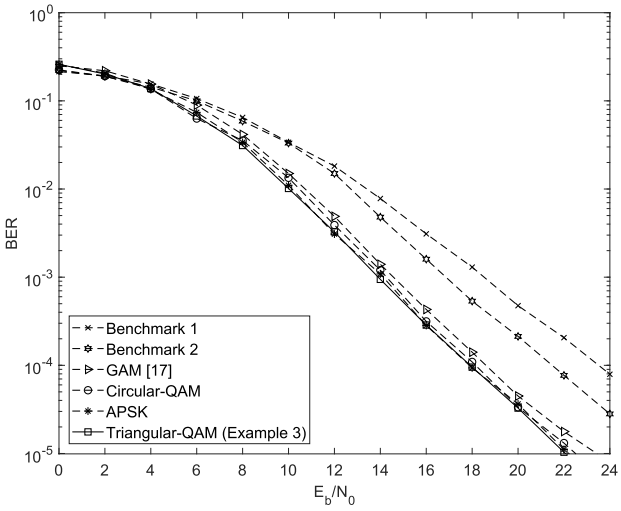

Fig. 5. BER performance versus the E_b/N_0 value for the uplink Rayleigh fading channel where $M = 8$.

the signal transmission on the uplink channel should be regarded as a space-time signal matrix, and then its error performance can be analyzed by using the metric Ψ, which is designed from the PD values, rather than using the metric $d_{\min}^{\mathrm{M}}$. A gain of 1 dB in the $\frac{E_b}{N_0}$ value can be observed at a BER of 10^{-5}, when compared to the scheme reported in [17].

For the high-rate codebook designs on the uplink fading channels, we consider the case using $M = 8$. Since it is difficult to identify suitable schemes for comparison from the literature, we have constructed two benchmark systems that are presented in Table II and Fig. 5. For Benchmarks 1 and 2, we use the same construction strategy as that of the proposed scheme, however, based on different signal sub-constellations. The PAM signals reported in [11] are utilized for Benchmark 1, while the star-QAM signals reported in [13] are utilized for Benchmark 2. Moreover, we have adopted three signal sub-constellations, which are referred to as the triangular-QAM (Fig. 6(b)), the circular-QAM (Fig. 6(c)), and amplitude-phase shift keying (APSK) (Fig. 6(d)) for the construction of the SCMA codebooks using the SEA. The three constellations

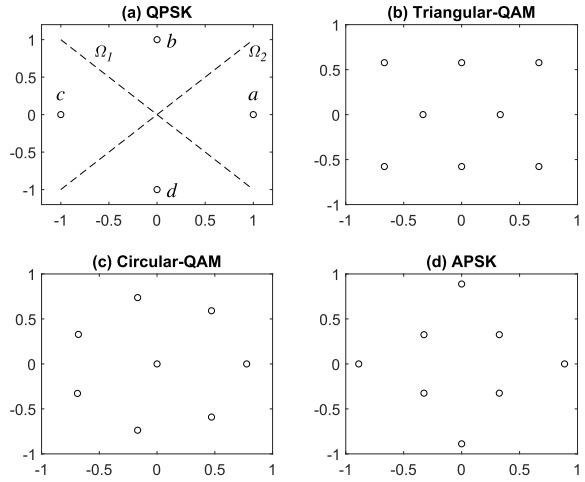

Fig. 6. Adopted signal sub-constellations.

TABLE III

COMPARISON OF VARIOUS SCHEMES CONSIDERING THE DOWNLINK RAYLEIGH FADING CHANNEL WHERE $M = 4$

codebook	$d_{\min}^{\mathrm{M}}$	$\Gamma_{\mathrm{DL}}^{(2)}$	$\Gamma_{\mathrm{DL}}^{(3)}$	$\Gamma_{\mathrm{DL}}^{(4)}$
Example 4	0.9195	0.1667	0.2276	0.0098
HUA [15]	0.707	0.3409	0.0897	0.0907
MD [11]	1.26	0.3517	0.707	1.7e+07
GAM [17]	0.7936	0.3583	0.116	2.56e+08
CR [14]	1.16	0.3776	1.25e+59	1.45e+90

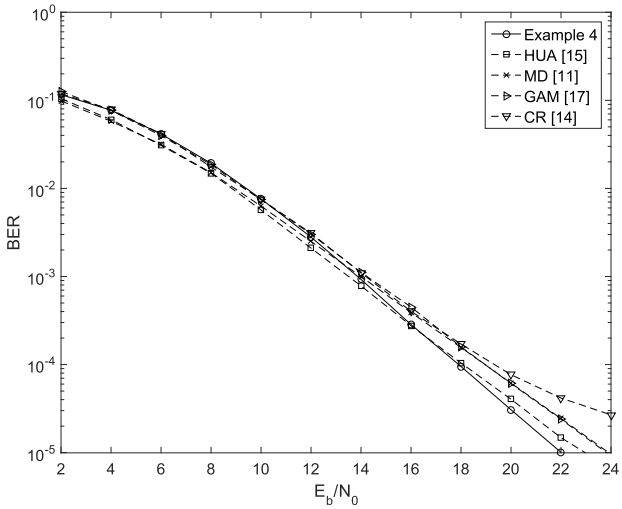

Fig. 7. BER performance versus the E_b/N_0 value for the downlink Rayleigh fading channel where $M = 4$.

guarantee similar MED values and a similar BER performance. A gain of 1.3 dB in the $\frac{E_b}{N_0}$ value can be observed at a BER of 10^{-5}, when comparing the proposed scheme given in Example 3 with the scheme reported in [17].

When considering the downlink Rayleigh fading channel where $M = 4$, Table III and Fig. 7 show that the level of the BER varies, following the same order as that of the $\Gamma_{\mathrm{DL}}^{(2)}$ values in the high-SNR region. For the scheme reported in [14], the design of the rotation angles has not been carefully investigated. This consequently leads to extremely large values

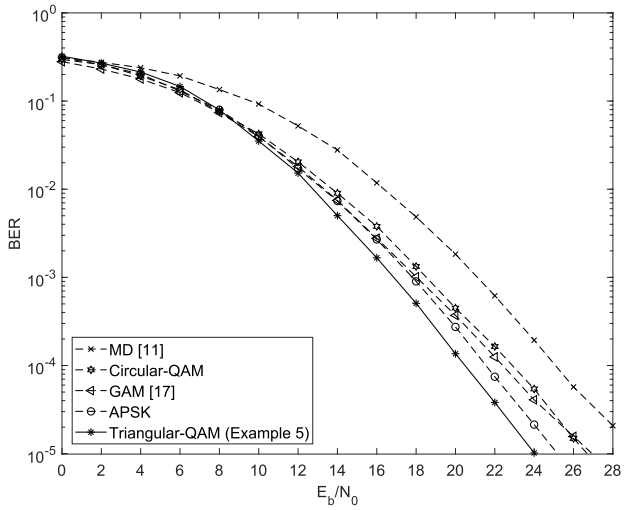

Fig. 8. BER performance versus the E_b/N_0 value for the downlink Rayleigh fading channel where $M = 8$.

for $\Gamma_{\mathrm{DL}}^{(3)}$ and $\Gamma_{\mathrm{DL}}^{(4)}$, which implies that some signal vector pairs where $\delta = 3$ or $\delta = 4$ are indistinguishable and have high pair-wise error probabilities. An error-floor phenomenon can be observed in the high-SNR region for the scheme reported in [14]. A gain of 1 dB in the $\frac{E_b}{N_0}$ value can be observed at a BER of 10^{-5}, when comparing the proposed scheme with the scheme reported in [15].

Lastly, for the high-rate case of $M = 8$, the related BER performance for the constructed schemes that consider the same sub-constellations depicted in Fig. 6(b)-(d) and the SEA is illustrated in Fig. 8. A gain of 3 dB in the $\frac{E_b}{N_0}$ value can be observed at a BER of 10^{-5}, when comparing the proposed scheme given in Example 5 with the scheme reported in [17].

VI. Conclusion

In this paper, we have proposed construction strategies for near-optimal SCMA codebooks under various channel environments. The design process includes the design for the rotation angles for signals from/for different UEs, the construction of codewords based on SUO and MUO, and the design for the labelling rules. The detailed design criteria and the related properties are derived and investigated. A low-complexity construction algorithm is then proposed for the codebook construction based on fading channels. Improved codebook designs for various channel conditions are provided. The design for cases that have large-scale SCMA parameters has become the target of our future research.

Appendix A
Proof of Proposition 1

We use the case where $K = 4$, $M = 4$, $d_{\mathrm{f}} = 3$ and $d_{\mathrm{v}} = 2$ for the determination of this proof. First, for the transmit signal vector, the minimum δ value is equal to $d_{\mathrm{v}} = 2$. The cases when $\delta = 2$ occur if, and only if, one of the UEs transmits two different codewords in $\mathbf{S}$ and $\hat{\mathbf{S}}$, respectively, while all of the other UEs transmit the same codeword.

Secondly, when $\delta = 3$, we assume that two of the UEs transmit two different codewords in $\mathbf{S}$ and $\hat{\mathbf{S}}$, respectively, while all of the other UEs transmit the same codeword. We further assume that the two UEs happen to share a single common RE. Without loss of generality, we let UE l_1 and UE l_2 be the two UEs, and REs k_1, k_2, and k_3 be the RE with different transmit signals. If we collect the three columns with different signals in $\mathbf{S}$ and $\hat{\mathbf{S}}$, we have

$$\mathbf{S}' = \begin{bmatrix} x_{l_1,k_1} & x_{l_1,k_2} & \varepsilon \\ \varepsilon & x_{l_2,k_2} & x_{l_2,k_3} \\ \varepsilon & \varepsilon & \varepsilon \end{bmatrix}, \quad \hat{\mathbf{S}}' = \begin{bmatrix} \hat{x}_{l_1,k_1} & \hat{x}_{l_1,k_2} & \varepsilon \\ \varepsilon & \hat{x}_{l_2,k_2} & \hat{x}_{l_2,k_3} \\ \varepsilon & \varepsilon & \varepsilon \end{bmatrix}, \tag{35}$$

$$d_{\mathrm{p}}^2(\mathbf{S}', \hat{\mathbf{S}}') = |x_{l_1,k_1} - \hat{x}_{l_1,k_1}|^2 |x_{l_1,k_2} - \hat{x}_{l_1,k_2}|^2 |x_{l_2,k_3} - \hat{x}_{l_2,k_3}|^2 + |x_{l_1,k_1} - \hat{x}_{l_1,k_1}|^2 |x_{l_2,k_2} - \hat{x}_{l_2,k_2}|^2 |x_{l_2,k_3} - \hat{x}_{l_2,k_3}|^2. \tag{36}$$

$$(d_{\mathrm{p},i,j,t_1,t_2,\cdots,t_L}^{\mathrm{M}})^2 = \prod_{k \in \rho\left(\mathbf{y}_{t_1,t_2,\cdots,t_L}^{(i)}, \mathbf{y}_{t_1,t_2,\cdots,t_L}^{(j)}\right)} |y_{k,t_1,t_2,\cdots,t_L}^{(i)} - y_{k,t_1,t_2,\cdots,t_L}^{(j)}|^2. \tag{37}$$

$$\mathcal{X}_1:\begin{bmatrix}-0.6667-0.5773i & 0.3333+0.0000i & 0.0000+0.0000i & 0.0000+0.0000i\\ 0.0000-0.5773i & -0.6667-0.5773i & 0.0000+0.0000i & 0.0000+0.0000i\\ -0.3333+0.0000i & -0.6667+0.5773i & 0.0000+0.0000i & 0.0000+0.0000i\\ 0.0000+0.5773i & 0.6667+0.5773i & 0.0000+0.0000i & 0.0000+0.0000i\\ -0.6667+0.5773i & 0.0000-0.5773i & 0.0000+0.0000i & 0.0000+0.0000i\\ 0.3333+0.0000i & 0.6667-0.5773i & 0.0000+0.0000i & 0.0000+0.0000i\\ 0.6667-0.5773i & 0.0000+0.5773i & 0.0000+0.0000i & 0.0000+0.0000i\\ 0.6667+0.5773i & -0.3333+0.0000i & 0.0000+0.0000i & 0.0000+0.0000i\end{bmatrix}^\top$$

$$\mathcal{X}_2:\begin{bmatrix}-0.6667-0.5773i & 0.0000+0.0000i & 0.3333+0.0000i & 0.0000+0.0000i\\ 0.0000-0.5773i & 0.0000+0.0000i & -0.6667-0.5773i & 0.0000+0.0000i\\ -0.3333+0.0000i & 0.0000+0.0000i & -0.6667+0.5773i & 0.0000+0.0000i\\ 0.0000+0.5773i & 0.0000+0.0000i & 0.6667+0.5773i & 0.0000+0.0000i\\ -0.6667+0.5773i & 0.0000+0.0000i & 0.0000-0.5773i & 0.0000+0.0000i\\ 0.3333+0.0000i & 0.0000+0.0000i & 0.6667-0.5773i & 0.0000+0.0000i\\ 0.6667-0.5773i & 0.0000+0.0000i & 0.0000+0.5773i & 0.0000+0.0000i\\ 0.6667+0.5773i & 0.0000+0.0000i & -0.3333+0.0000i & 0.0000+0.0000i\end{bmatrix}^\top$$

$$\mathcal{X}_3:\begin{bmatrix}-0.6667-0.5773i & 0.0000+0.0000i & 0.0000+0.0000i & 0.3333+0.0000i\\ 0.0000-0.5773i & 0.0000+0.0000i & 0.0000+0.0000i & -0.6667-0.5773i\\ -0.3333+0.0000i & 0.0000+0.0000i & 0.0000+0.0000i & -0.6667+0.5773i\\ 0.0000+0.5773i & 0.0000+0.0000i & 0.0000+0.0000i & 0.6667+0.5773i\\ -0.6667+0.5773i & 0.0000+0.0000i & 0.0000+0.0000i & 0.0000-0.5773i\\ 0.3333+0.0000i & 0.0000+0.0000i & 0.0000+0.0000i & 0.6667-0.5773i\\ 0.6667-0.5773i & 0.0000+0.0000i & 0.0000+0.0000i & 0.0000+0.5773i\\ 0.6667+0.5773i & 0.0000+0.0000i & 0.0000+0.0000i & -0.3333+0.0000i\end{bmatrix}^\top$$

$$\mathcal{X}_4:\begin{bmatrix}0.0000+0.0000i & -0.6667-0.5773i & 0.3333+0.0000i & 0.0000+0.0000i\\ 0.0000+0.0000i & 0.0000-0.5773i & -0.6667-0.5773i & 0.0000+0.0000i\\ 0.0000+0.0000i & -0.3333+0.0000i & -0.6667+0.5773i & 0.0000+0.0000i\\ 0.0000+0.0000i & 0.0000+0.5773i & 0.6667+0.5773i & 0.0000+0.0000i\\ 0.0000+0.0000i & -0.6667+0.5773i & 0.0000-0.5773i & 0.0000+0.0000i\\ 0.0000+0.0000i & 0.3333+0.0000i & 0.6667-0.5773i & 0.0000+0.0000i\\ 0.0000+0.0000i & 0.6667-0.5773i & 0.0000+0.5773i & 0.0000+0.0000i\\ 0.0000+0.0000i & 0.6667+0.5773i & -0.3333+0.0000i & 0.0000+0.0000i\end{bmatrix}^\top$$

$$\mathcal{X}_5:\begin{bmatrix}0.0000+0.0000i & -0.6667-0.5773i & 0.0000+0.0000i & 0.3333+0.0000i\\ 0.0000+0.0000i & 0.0000-0.5773i & 0.0000+0.0000i & -0.6667-0.5773i\\ 0.0000+0.0000i & -0.3333+0.0000i & 0.0000+0.0000i & -0.6667+0.5773i\\ 0.0000+0.0000i & 0.0000+0.5773i & 0.0000+0.0000i & 0.6667+0.5773i\\ 0.0000+0.0000i & -0.6667+0.5773i & 0.0000+0.0000i & 0.0000-0.5773i\\ 0.0000+0.0000i & 0.3333+0.0000i & 0.0000+0.0000i & 0.6667-0.5773i\\ 0.0000+0.0000i & 0.6667-0.5773i & 0.0000+0.0000i & 0.0000+0.5773i\\ 0.0000+0.0000i & 0.6667+0.5773i & 0.0000+0.0000i & -0.3333+0.0000i\end{bmatrix}^\top$$

$$\mathcal{X}_6:\begin{bmatrix}0.0000+0.0000i & 0.0000+0.0000i & -0.6667-0.5773i & 0.3333+0.0000i\\ 0.0000+0.0000i & 0.0000+0.0000i & 0.0000-0.5773i & -0.6667-0.5773i\\ 0.0000+0.0000i & 0.0000+0.0000i & -0.3333+0.0000i & -0.6667+0.5773i\\ 0.0000+0.0000i & 0.0000+0.0000i & 0.0000+0.5773i & 0.6667+0.5773i\\ 0.0000+0.0000i & 0.0000+0.0000i & -0.6667+0.5773i & 0.0000-0.5773i\\ 0.0000+0.0000i & 0.0000+0.0000i & 0.3333+0.0000i & 0.6667-0.5773i\\ 0.0000+0.0000i & 0.0000+0.0000i & 0.6667-0.5773i & 0.0000+0.5773i\\ 0.0000+0.0000i & 0.0000+0.0000i & 0.6667+0.5773i & -0.3333+0.0000i\end{bmatrix}^\top$$

where we use the symbol ε to denote the positions in which $\mathbf{S}'$ and $\hat{\mathbf{S}}'$ have the same values. Consequently, we obtain a signal vector pair that has a δ value of 3. If we calculate the d_{p}^2 value between $\mathbf{S}'$ and $\hat{\mathbf{S}}'$, we can obtain (36) as shown at the bottom of page 10.

In those cases that consider the AWGN channel, the reason for performing the rotation angle design is because it affects the MED values for the combined signal vectors. However, for the uplink Rayleigh fading channel, the design metric is related to the PD values rather than the ED values. It is shown in (36) that for each squared ED term, e.g., $|x_{l_1,k_1}-\hat{x}_{l_1,k_1}|^2$, the signals x_{l_1,k_1} and $\hat{x}_{l_1,k_1}$ are actually sourced from the same user and have the same phase shift value. Consequently, this term can be re-write as $|e^{j\phi_{l_1,k_1}}|^2|c_{l_1,k_1}-\hat{c}_{l_1,k_1}|^2$, where $|e^{j\phi_{l_1,k_1}}|^2$ is always equal to 1. Accordingly, phase rotations for different users does not change the value reported in (36) and can be omitted. This proof holds for all possible δ values.

$$\mathcal{X}_1:\begin{bmatrix}0.7071+0.7071i & 0.7071-0.7071i & -0.7071+0.7071i & -0.7071-0.7071i\\ 0.0891-0.9960i & 0.9960+0.0891i & -0.0891+0.9960i & -0.9960-0.0891i\\ 0.0000+0.0000i & 0.0000+0.0000i & 0.0000+0.0000i & 0.0000+0.0000i\\ 0.0000+0.0000i & 0.0000+0.0000i & 0.0000+0.0000i & 0.0000+0.0000i\end{bmatrix}$$

$$\mathcal{X}_2:\begin{bmatrix}-0.9960-0.0891i & -0.0891+0.9960i & 0.0891-0.9960i & 0.9960+0.0891i\\ 0.0000+0.0000i & 0.0000+0.0000i & 0.0000+0.0000i & 0.0000+0.0000i\\ -0.4246+0.9054i & -0.9054-0.4246i & 0.4246-0.9054i & 0.9054+0.4246i\\ 0.0000+0.0000i & 0.0000+0.0000i & 0.0000+0.0000i & 0.0000+0.0000i\end{bmatrix}$$

$$\mathcal{X}_3:\begin{bmatrix}-0.9054-0.4246i & -0.4246+0.9054i & 0.4246-0.9054i & 0.9054+0.4246i\\ 0.0000+0.0000i & 0.0000+0.0000i & 0.0000+0.0000i & 0.0000+0.0000i\\ 0.0000+0.0000i & 0.0000+0.0000i & 0.0000+0.0000i & 0.0000+0.0000i\\ 0.7071-0.7071i & -0.7071-0.7071i & -0.7071+0.7071i & 0.7071+0.7071i\end{bmatrix}$$

$$\mathcal{X}_4:\begin{bmatrix}0.0000+0.0000i & 0.0000+0.0000i & 0.0000+0.0000i & 0.0000+0.0000i\\ -0.9054-0.4246i & -0.4246+0.9054i & 0.4246-0.9054i & 0.9054+0.4246i\\ -0.7071+0.7071i & 0.7071+0.7071i & 0.7071-0.7071i & -0.7071-0.7071i\\ 0.0000+0.0000i & 0.0000+0.0000i & 0.0000+0.0000i & 0.0000+0.0000i\end{bmatrix}$$

$$\mathcal{X}_5:\begin{bmatrix}0.0000+0.0000i & 0.0000+0.0000i & 0.0000+0.0000i & 0.0000+0.0000i\\ 0.7071+0.7071i & 0.7071-0.7071i & -0.7071+0.7071i & -0.7071-0.7071i\\ 0.0000+0.0000i & 0.0000+0.0000i & 0.0000+0.0000i & 0.0000+0.0000i\\ 0.9960+0.0891i & -0.0891+0.9960i & -0.9960-0.0891i & 0.0891-0.9960i\end{bmatrix}$$

$$\mathcal{X}_6:\begin{bmatrix}0.0000+0.0000i & 0.0000+0.0000i & 0.0000+0.0000i & 0.0000+0.0000i\\ 0.0000+0.0000i & 0.0000+0.0000i & 0.0000+0.0000i & 0.0000+0.0000i\\ -0.9960-0.0891i & -0.0891+0.9960i & 0.0891-0.9960i & 0.9960+0.0891i\\ -0.4246+0.9054i & 0.4246-0.9054i & 0.9054+0.4246i & -0.9054-0.4246i\end{bmatrix}$$

APPENDIX B
PROOF OF PROPOSITION 2

We first prove the following lemma:

Lemma 1: Assume that a signal sub-constellation, which is symmetrical with respect to an axis that passes the origin on the two-dimensional signal space, is adopted. If we swap the signals on one of the d_{v} dimensions of a codebook that achieves a specific Ψ value given in (26) with respect to the symmetry axis, we are able to produce another codebook which has the same Ψ value, the same codeword spectrum (i.e., the possible PD values and the number of the codeword pairs with the same PD value), and also the same squared ED value on each dimension of a single codeword pair.

Proof: We use an example which considers $M=4$, $d_{\mathrm{v}}=2$, and the QPSK signal illustrated in Fig. 6(a) for the determination of this proof. Assume that we have a size-4 codebook

$$\begin{bmatrix}a & c & b & d\\ d & b & c & a\end{bmatrix}. \tag{38}$$

There are two possible cases for the symmetry axes for the QPSK signal sub-constellation. The first is the y-axis (or x-axis). For this case, we fix the signal points b and d, and swap points a and c on the second dimension of (38). For the codeword pair $\{(b,c)^\top,(d,a)^\top\}$ from the original codebook, if we swap c and a on the second dimension, we obtain $\{(b,a)^\top,(d,c)^\top\}$. It is found that the squared ED value on the second dimension remains the same, and the new codeword pair has exactly the same PD value as that of the original. In addition, for the two codeword pairs $\{(c,b)^\top,(d,a)^\top\}$ and $\{(c,b)^\top,(b,c)^\top\}$, if we swap c and a on the second dimension, we obtain $\{(c,b)^\top,(d,c)^\top\}$ and $\{(c,b)^\top,(b,a)^\top\}$. However, the squared ED value between points b and a is exactly the same as that between b and c. Consequently, the two new codeword pairs still maintain the same PD values as those of the original pairs. All possible codeword pairs that involve the change in signal points have been included in the above-mentioned two cases.

The other possible symmetry axis is the line Ω_1 (or Ω_2) illustrated in Fig. 6(a). In this case, we swap b with c and a with d. Consequently, for the codeword pair $\{(a,d)^\top,(d,a)^\top\}$ from the original codebook, we obtain the new pair $\{(a,a)^\top,(d,d)^\top\}$. It is found that the squared ED value on the second dimension remains the same, and the new codeword pair has exactly the same PD value as that of the original. In addition, for the codeword pair $\{(a,d)^\top,(c,b)^\top\}$ from the original codebook, we obtain the new pair $\{(a,a)^\top,(c,c)^\top\}$. However, the squared ED value between points d and b is exactly the same as that between a and c. Consequently, the new codeword pair still maintains the same PD value as that of the original. All possible cases

$$\mathcal{X}_1:\begin{bmatrix} 0.3333+0.0000i & -0.8000+0.3712i & 0.0000+0.0000i & 0.0000+0.0000i \\ 0.0000+0.5773i & 0.4817+0.7387i & 0.0000+0.0000i & 0.0000+0.0000i \\ -0.3333+0.0000i & 0.8000-0.3712i & 0.0000+0.0000i & 0.0000+0.0000i \\ -0.6667-0.5773i & -0.1591+0.5550i & 0.0000+0.0000i & 0.0000+0.0000i \\ -0.6667+0.5773i & -0.3204-0.0919i & 0.0000+0.0000i & 0.0000+0.0000i \\ 0.0000-0.5773i & -0.4817-0.7387i & 0.0000+0.0000i & 0.0000+0.0000i \\ 0.6667-0.5773i & 0.3204+0.0919i & 0.0000+0.0000i & 0.0000+0.0000i \\ 0.6667+0.5773i & 0.1591-0.5550i & 0.0000+0.0000i & 0.0000+0.0000i \end{bmatrix}^\top$$

$$\mathcal{X}_2:\begin{bmatrix} 0.3204+0.0919i & 0.0000+0.0000i & -0.8808+0.0445i & 0.0000+0.0000i \\ -0.1591+0.5550i & 0.0000+0.0000i & 0.1699+0.8654i & 0.0000+0.0000i \\ -0.3204-0.0919i & 0.0000+0.0000i & 0.8808-0.0445i & 0.0000+0.0000i \\ -0.4817-0.7387i & 0.0000+0.0000i & -0.3554+0.4549i & 0.0000+0.0000i \\ -0.8000+0.3712i & 0.0000+0.0000i & -0.2627-0.2052i & 0.0000+0.0000i \\ 0.1591-0.5550i & 0.0000+0.0000i & -0.1699-0.8654i & 0.0000+0.0000i \\ 0.8000-0.3712i & 0.0000+0.0000i & 0.2627+0.2052i & 0.0000+0.0000i \\ 0.4817+0.7387i & 0.0000+0.0000i & 0.3554-0.4549i & 0.0000+0.0000i \end{bmatrix}^\top$$

$$\mathcal{X}_3:\begin{bmatrix} 0.2627+0.2052i & 0.0000+0.0000i & 0.0000+0.0000i & -0.6667+0.5773i \\ -0.3554+0.4549i & 0.0000+0.0000i & 0.0000+0.0000i & 0.6667+0.5773i \\ -0.2627-0.2052i & 0.0000+0.0000i & 0.0000+0.0000i & 0.6667-0.5773i \\ -0.1699-0.8654i & 0.0000+0.0000i & 0.0000+0.0000i & 0.0000+0.5773i \\ -0.8808+0.0445i & 0.0000+0.0000i & 0.0000+0.0000i & -0.3333+0.0000i \\ 0.3554-0.4549i & 0.0000+0.0000i & 0.0000+0.0000i & -0.6667-0.5773i \\ 0.8808-0.0445i & 0.0000+0.0000i & 0.0000+0.0000i & 0.3333+0.0000i \\ 0.1699+0.8654i & 0.0000+0.0000i & 0.0000+0.0000i & 0.0000-0.5773i \end{bmatrix}^\top$$

$$\mathcal{X}_4:\begin{bmatrix} 0.0000+0.0000i & 0.2627+0.2052i & -0.6667+0.5773i & 0.0000+0.0000i \\ 0.0000+0.0000i & -0.3554+0.4549i & 0.6667+0.5773i & 0.0000+0.0000i \\ 0.0000+0.0000i & -0.2627-0.2052i & 0.6667-0.5773i & 0.0000+0.0000i \\ 0.0000+0.0000i & -0.1699-0.8654i & 0.0000+0.5773i & 0.0000+0.0000i \\ 0.0000+0.0000i & -0.8808+0.0445i & -0.3333+0.0000i & 0.0000+0.0000i \\ 0.0000+0.0000i & 0.3554-0.4549i & -0.6667-0.5773i & 0.0000+0.0000i \\ 0.0000+0.0000i & 0.8808-0.0445i & 0.3333+0.0000i & 0.0000+0.0000i \\ 0.0000+0.0000i & 0.1699+0.8654i & 0.0000-0.5773i & 0.0000+0.0000i \end{bmatrix}^\top$$

$$\mathcal{X}_5:\begin{bmatrix} 0.0000+0.0000i & 0.3333+0.0000i & 0.0000+0.0000i & -0.8000+0.3712i \\ 0.0000+0.0000i & 0.0000+0.5773i & 0.0000+0.0000i & 0.4817+0.7387i \\ 0.0000+0.0000i & -0.3333+0.0000i & 0.0000+0.0000i & 0.8000-0.3712i \\ 0.0000+0.0000i & -0.6667-0.5773i & 0.0000+0.0000i & -0.1591+0.5550i \\ 0.0000+0.0000i & -0.6667+0.5773i & 0.0000+0.0000i & -0.3204-0.0919i \\ 0.0000+0.0000i & 0.0000-0.5773i & 0.0000+0.0000i & -0.4817-0.7387i \\ 0.0000+0.0000i & 0.6667-0.5773i & 0.0000+0.0000i & 0.3204+0.0919i \\ 0.0000+0.0000i & 0.6667+0.5773i & 0.0000+0.0000i & 0.1591-0.5550i \end{bmatrix}^\top$$

$$\mathcal{X}_6:\begin{bmatrix} 0.0000+0.0000i & 0.0000+0.0000i & 0.3204+0.0919i & -0.8808+0.0445i \\ 0.0000+0.0000i & 0.0000+0.0000i & -0.1591+0.5550i & 0.1699+0.8654i \\ 0.0000+0.0000i & 0.0000+0.0000i & -0.3204-0.0919i & 0.8808-0.0445i \\ 0.0000+0.0000i & 0.0000+0.0000i & -0.4817-0.7387i & -0.3554+0.4549i \\ 0.0000+0.0000i & 0.0000+0.0000i & -0.8000+0.3712i & -0.2627-0.2052i \\ 0.0000+0.0000i & 0.0000+0.0000i & 0.1591-0.5550i & -0.1699-0.8654i \\ 0.0000+0.0000i & 0.0000+0.0000i & 0.8000-0.3712i & 0.2627+0.2052i \\ 0.0000+0.0000i & 0.0000+0.0000i & 0.4817+0.7387i & 0.3554-0.4549i \end{bmatrix}^\top$$

for the codeword pairs that involve the change in signal points have been included in the above-mentioned two cases. Since all the codeword pairs maintain the same PD value after the swap, The new codebook which has the same spectrum, and, hence, achieves the same Ψ value. This proof also holds for larger values of M and d_{v}. ■

When a codebook that achieves the best Ψ value has been searched based on SUO, and if we use a symmetrical signal sub-constellation, it is easy to obtain several codebooks that have the same optimal Ψ value and the same spectrum according to Lemma 1. We may intend to preserve these codebooks for the design process based on MUO. However, when calculating the PD value for the signal vector pairs that consider multiple users, e.g., the case given in (36) where $\delta = 3$, if we change the codebook for a single user, for each codeword pair in the original codebook, we can always identify the corresponding codeword pair in the new codebook that has exactly the same squared ED values on each dimension, and, hance, produces the same value for (36). Consequently, changing the mother codebooks for a single user not only does not change the PD value, but also does not change the spectrum of the signal vectors when $\delta = 3$. Similar results can be shown when $\delta > 3$. Consequently, we conclude that the process for the codebook design based on MUO can be omitted for the uplink Rayleigh fading channels.

APPENDIX C
DESIGNED SCMA CODEBOOKS

For the case where $M = 4$, the four columns of a matrix represent the codewords labelled by 00, 01, 10, and 11, respectively. Similarly, for the case where $M = 8$, the eight columns represent the codewords labelled by 000, 001, 010, 011, 100, 101, 110, and 111, respectively.

A. Codebooks for Example 1 Where There Are 6 UEs, 4 REs and $M = 4$

$\mathcal{X}_1$–$\mathcal{X}_6$, as shown at the top of the page 10.

B. Codebooks for Example 2 Where There Are 6 UEs, 4 REs and $M = 4$

$\mathcal{X}_1$–$\mathcal{X}_6$, as shown at the bottom of the page 10.

C. Codebooks for Example 3 Where There Are 6 UEs, 4 REs and $M = 8$

$\mathcal{X}_1$–$\mathcal{X}_6$, as shown at the top of the page 11.

D. Codebooks for Example 4 Where There Are 6 UEs, 4 REs and $M = 4$

$\mathcal{X}_1$–$\mathcal{X}_6$, as shown at the bottom of the page 11.

E. Codebooks for Example 5 Where There Are 6 UEs, 4 REs and $M = 8$

$\mathcal{X}_1$–$\mathcal{X}_6$, as shown at the top of the page 12.

REFERENCES

[1] A. Osseiran *et al.*, "Scenarios for 5G mobile and wireless communications: The vision of the METIS project," *IEEE Commun. Mag.*, vol. 52, no. 5, pp. 26–35, May 2014.

[2] L. Dai, B. Wang, Z. Ding, Z. Wang, S. Chen, and L. Hanzo, "A survey of non-orthogonal multiple access for 5G," *IEEE Commun. Surveys Tuts.*, vol. 20, no. 3, pp. 2294–2323, Jul./Sep. 2018.

[3] S. M. R. Islam, N. Avazov, O. A. Dobre, and K.-S. Kwak, "Power-domain non-orthogonal multiple access (NOMA) in 5G systems: Potentials and challenges," *IEEE Commun. Surveys Tuts.*, vol. 19, no. 2, pp. 721–742, Apr./Jun. 2017.

[4] R. Hoshyar, F. P. Wathan, and R. Tafazolli, "Novel low-density signature for synchronous CDMA systems over AWGN channel," *IEEE Trans. Signal Process.*, vol. 56, no. 4, pp. 1616–1626, Apr. 2008.

[5] R. Hoshyar, R. Razavi, and M. Al-Imari, "LDS-OFDM an efficient multiple access technique," in *Proc. IEEE 71st Veh. Technol. Conf.*, May 2010, pp. 1–5.

[6] Z. Yuan, G. Yu, W. Li, Y. Yuan, X. Wang, and J. Xu, "Multi-user shared access for Internet of Things," in *Proc. IEEE 83rd Veh. Technol. Conf. (VTC Spring)*, May 2016, pp. 1–5.

[7] Z. Li and W. Chen, "Sparse code multiple access," in *Proc. IEEE 24th Int. Symp. Pers. Indoor Mobile Radio Commun. (PIMRC)*, Sep. 2013, pp. 332–336.

[8] M. Taherzadeh, H. Nikopour, A. Bayesteh, and H. Baligh, "SCMA codebook design," in *Proc. IEEE 80th Veh. Technol. Conf. (VTC-Fall)*, Vancouver, BC, Canada, Sep. 2014, pp. 1–5.

[9] S. Tang, L. Hao, and Z. Ma, "Low complexity joint MPA detection for downlink MIMO-SCMA," in *Proc. IEEE Global Commun. Conf. (GLOBECOM)*, Washington, DC, USA, Dec. 2016, pp. 1–4.

[10] A. Ghaffari, M. Leonardon, Y. Savaria, C. Jego, and C. Leroux, "Improving performance of SCMA MPA decoders using estimation of conditional probabilities," in *Proc. 15th IEEE Int. New Circuits Syst. Conf. (NEWCAS)*, Strasbourg, France, Jun. 2017, pp. 21–24.

[11] D. Cai, P. Fan, X. Lei, Y. Liu, and D. Chen, "Multi-dimensional SCMA codebook design based on constellation rotation and interleaving," in *Proc. IEEE 83rd Veh. Technol. Conf. (VTC Spring)*, Nanjing, China, May 2016, pp. 1–5.

[12] S. Zhang *et al.*, "A capacity-based codebook design method for sparse code multiple access systems," in *Proc. 8th Int. Conf. Wireless Commun. Signal Process. (WCSP)*, Yangzhou, China, Oct. 2016, pp. 1–5.

[13] L. Yu, X. Lei, P. Fan, and D. Chen, "An optimized design of SCMA codebook based on star-QAM signaling constellations," in *Proc. Int. Conf. Wireless Commun. Signal Process. (WCSP)*, Nanjing, China, Oct. 2015, pp. 1–5.
[14] Y. Zhou, Q. Yu, W. Meng, and C. Li, "SCMA codebook design based on constellation rotation," in *Proc. IEEE Int. Conf. Commun.(ICC)*, Paris, France, May 2017, pp. 21–25.
[15] Altera Innovate Asia. Presentation. *1st 5G Algorithm Innovation Competition-ENV1.0-SCMA*. [Online]. Available: http://www.innovateasia.com/5g/en/gp2.html
[16] S. Liu, J. Wang, J. Bao, and C. Liu, "Optimized SCMA codebook design by QAM constellation segmentation with maximized MED," *IEEE Access*, vol. 6, pp. 63232–63242, 2018.
[17] Z. Mheich, L. Wen, P. Xiao, and A. Maaref, "Design of SCMA codebooks based on golden angle modulation," *IEEE Trans. Veh. Technol.*, vol. 68, no. 2, pp. 1501–1509, Feb. 2019.
[18] V. Tarokh, N. Seshadri, and A. R. Calderbank, "Space-time codes for high data rate wireless communication: Performance criterion and code construction," *IEEE Trans. Inf. Theory*, vol. 44, no. 2, pp. 744–765, Mar. 1998.
[19] J. Yuan, Z. Chen, B. Vucetic, and W. Firmanto, "Performance and design of space-time coding in fading channels," *IEEE Trans. Commun.*, vol. 51, no. 12, pp. 1991–1996, Dec. 2003.
[20] Z. Safar and K. J. R. Liu, "Performance analysis of space-time codes over correlated Rayleigh fading channels," in *Proc. IEEE Int. Conf. Commun. (ICC)*, Anchorage, AK, USA, vol. 5, May 2003, pp. 3185–3189.
[21] D. Divsalar and M. K. Simon, "The design of trellis coded MPSK for fading channels: Performance criteria," *IEEE Trans. Commun.*, vol. COM-36, no. 9, pp. 1004–1012, Sep. 1988.
[22] F. R. Kschischang, B. J. Frey, and H.-A. Loeliger, "Factor graphs and the sum-product algorithm," *IEEE Trans. Inf. Theory*, vol. 47, no. 2, pp. 498–519, Feb. 2001.
[23] H. Loeliger, "An Introduction to factor graphs," *IEEE Signal Process. Mag.*, vol. 21, no. 1, pp. 28–41, Jan. 2004.
[24] E. Agrell, J. Lassing, E. G. Strom, and T. Ottosson, "The binary reflected gray code is optimal for M-PSK," in *Proc. Int. Symp. Inf. Theory (ISIT)*, Chicago, IL, USA, Dec. 2004, p. 164.
[25] L. Wang, D. Xu, and X. Zhang, "Recursive bit metric generation for PSK signals with gray labeling," *IEEE Commun. Lett.*, vol. 16, no. 2, pp. 180–182, Feb. 2012.
[26] F. Schreckenbach, N. Gortz, J. Hagenauer, and G. Bauch, "Optimization of symbol mappings for bit-interleaved coded Modulation with iterative decoding," *IEEE Commun. Lett.*, vol. 7, no. 12, pp. 593–595, Dec. 2003.
[27] K. Zeger and A. Gersho, "Pseudo-gray coding," *IEEE Trans. Commun.*, vol. 38, no. 12, pp. 2147–2158, Dec. 1990.
[28] Y. Zhang *et al.*, "Constant modulus codebook design for SCMA system," in *Proc. IEEE Int. Conf. Commun. Syst. (ICCS)*, Chengdu, China, Dec. 2018, pp. 242–246.
[29] L. Tian, J. Zhong, M. Zhao, and L. Wen, "A suboptimal algorithm for SCMA codebook design over uplink Rayleigh fading channels," in *Proc. IEEE 87th Veh. Technol. Conf. (VTC Spring)*, Jun. 2018, pp. 1–5.

Yen-Ming Chen (Member, IEEE) received the B.S. degree in electrical and control engineering from National Chiao Tung University, Hsinchu, Taiwan, in 2004, the M.S. degree (Hons.) in communications engineering from National Central University, Jhongli, Taiwan, in 2006, and the Ph.D. degree in electrical engineering from National Tsing Hua University (NTHU), Hsinchu, in 2011.

From 2011 to 2014, he was a Post-Doctoral Fellow with the Department of Electrical Engineering, NTHU. From 2014 to 2016, he was an Assistant Professor with the Department of Electronic Engineering, Chung Yuan Christian University. In 2017, he joined the Faculty of National Sun Yat-sen University, Kaohsiung, where he is currently an Assistant Professor with the Institute of Communications Engineering and also with the Department of Electrical Engineering. His current research interests include error-correcting codes, wireless communications, non-orthogonal multiple access, and biometrics.

Jian-Wei Chen received the B.S. degree in electrical engineering from Tamkang University, Tamsui, Taiwan, in 2017, and the M.S. degree in communications engineering from National Sun Yat-sen University, Kaohsiung, Taiwan, in 2019. He is currently with the Realtek Semiconductor Corporation, Hsinchu, Taiwan. His research interests include wireless communication, non-orthogonal multiple access, and error-correcting codes.